



Original

Preventive effect of Ninjin-yoei-to, a Kampo medicine, on amyloid β_{1-42} -induced neurodegeneration via intracellular Zn^{2+} toxicity in the dentate gyrus

Haruna TAMANO, Haruna TOKORO, Daichi MURAKAMI, Ryo FURUHATA, Satoko NAKAJIMA, Nana SAEKI, Misa KATAHIRA, Aoi SHIOYA, Yukino TANAKA, Mako EGAWA and Atsushi TAKEDA

Department of Neurophysiology, School of Pharmaceutical Sciences, University of Shizuoka, 52-1 Yada, Suruga-ku, Shizuoka 422-8526, Japan

Abstract: Ninjin-yoei-to (NYT), a Kampo medicine, has ameliorative effects on cognitive dysfunction via enhancing cholinergic neuron activity. To explore an efficacy of NYT administration for prevention and cure of Alzheimer's disease, here we examined the effect of NYT on amyloid β_{1-42} ($A\beta_{1-42}$)-induced neurodegeneration in the dentate gyrus. A diet containing 3% NYT was administered to mice for 2 weeks and human $A\beta_{1-42}$ was intracerebroventricularly injected. Neurodegeneration in the dentate granule cell layer of the hippocampus, which was determined 2 weeks after the injection, was rescued by administration of the diet for 4 weeks. $A\beta$ staining (uptake) was not modified in the dentate granule cell layer by pre-administration of the diet for 2 weeks, while $A\beta_{1-42}$ -induced increase in intracellular Zn^{2+} was reduced, suggesting that pre-administration of NYT prior to $A\beta$ injection is effective for reducing $A\beta_{1-42}$ -induced Zn^{2+} toxicity in the dentate gyrus. As a matter of fact, $A\beta_{1-42}$ -induced neurodegeneration in the dentate gyrus was rescued by pre-administration of NYT. Interestingly, the level of metallothioneins, intracellular Zn^{2+} -binding proteins, which can capture Zn^{2+} from Zn - $A\beta_{1-42}$ complexes, was elevated in the dentate granule cell layer by pre-administration of NYT. The present study suggests that pre-administration of NYT prevents $A\beta_{1-42}$ -mediated neurodegeneration in the dentate gyrus by induced synthesis of metallothioneins, which reduces intracellular Zn^{2+} toxicity induced by $A\beta_{1-42}$.

Key words: Alzheimer's disease, amyloid β_{1-42} , metallothionein, Ninjin-yoei-to, Zn^{2+} dysregulation

Introduction

In the early stage of Alzheimer's disease (AD), substantial synaptic and neuronal losses are observed when hippocampus-dependent memory loss becomes clinically detectable [1, 2]. The entorhinal cortex and the dentate gyrus are vulnerable to AD and aging, respectively [3]. The perforant pathway from the entorhinal cortex innervates dentate granule cells and is one of the earliest and most severely affected pathways in the brain of the patients with AD [4–6], suggesting that the cellular disconnection from the entorhinal cortex to the dentate gyrus is associated with the AD development. In

elderly persons with mild cognitive impairment prior to AD [7], approximately 30% fewer neurons are observed in the entorhinal cortex and correlate with hippocampus-dependent cognitive impairment [1, 4]. Therefore, dentate granule cell degeneration may be a target for the defense strategy against the AD development.

It has been considered that neuronal accumulation of amyloid β ($A\beta$) is an upstream event in the AD pathogenesis. When the extracellular concentration of human $A\beta_{1-42}$ reaches high picomolar (>100 pM) in the rat hippocampus, Zn - $A\beta_{1-42}$ complexes are rapidly formed in the extracellular compartment. They are preferentially taken up into dentate granule cells followed by $A\beta_{1-42}$ -induced

(Received 4 March 2021 / Accepted 31 May 2021 / Published online in J-STAGE 29 June 2021)

Corresponding author: A. Takeda. e-mail: takedaa@u-shizuoka-ken.ac.jp



This is an open-access article distributed under the terms of the Creative Commons Attribution Non-Commercial No Derivatives (by-nc-nd) License <<http://creativecommons.org/licenses/by-nc-nd/4.0/>>.

intracellular Zn²⁺ dysregulation in dentate granule cells [8–10]. Because the basal concentration of intracellular Zn²⁺ is extremely low (~100 pM) [11, 12], Zn²⁺ is readily released from intracellular A β ₁₋₄₂ complexes, resulting in A β ₁₋₄₂-induced intracellular Zn²⁺ toxicity that causes neurodegeneration [13].

With regard to Japanese herbal (Kampo) medicines associated with AD therapy, it has been reported that Yokukansan (YKS) is effective to improve behavioral and psychological symptoms of dementia (BPSD) such as aggression, hallucinations, disturbed behavior and agitation [14–16]. However, it is not well recognized whether YKS is effective for core symptoms such as cognitive deficits [17]. In patients with AD who are treated with donepezil, a cholinesterase inhibitor and/or Ninjin-yoei-to (NYT) over a 2-year period, on the other hand, donepezil and NYT treatments show an improved cognitive outcome and alleviation of AD-related depression [18]. Unfortunately, the effect of NYT itself has not been tested in the study. In cultured basal forebrain neurons, NYT elevates choline acetyltransferase activity [19]. NYT improves the memory deficits in ovariectomized mice [20], and also improves scopolamine-induced impairment of passive avoidance response by enhancing the cholinergic system [21]. AD and aging are associated with reduced activity of choline acetyltransferase and cholinergic neurodegeneration in the central nervous system [22–24]. It has been reported that cholinesterase inhibitors, e.g., donepezil are effective in the treatment of the patients with AD [25–27]. On the basis of these findings, it is considered that NYT has potential therapeutic effects for the treatment of the patients with AD.

On the other hand, it is unknown whether NYT is effective for A β ₁₋₄₂-induced intracellular Zn²⁺ dysregulation followed by neurodegeneration. We postulated a protective effect of NYT via the induction of metallothioneins (MTs), Zn²⁺-binding proteins on A β ₁₋₄₂ neurotoxicity. In the present study, we examined whether NYT protects A β ₁₋₄₂-induced neurodegeneration in the dentate gyrus, which was induced after intracerebroventricular injection of A β ₁₋₄₂ into mice, focused on rescuing intracellular Zn²⁺ dysregulation induced by A β ₁₋₄₂.

Material and Methods

NYT-containing diet and chemicals

NYT was obtained in the form of dried powder extract from Tsumura & Co. (Tokyo, Japan). This drug was manufactured from a mixture of *Angelicae radix* (4.0 g, root of *Angelica acutiloba* Kitagawa), *Hoelen* (4.0 g, fungus of *Poria cocos* Wolf), *Rehmanniae radix* (4.0 g,

root of *Rehmannia glutinosa* Lib., var. *purpurea* Mak), *Atractylodis rhizoma* (4.0 g, root of *Atractylodes japonica* Koidzumi), *Ginseng radix* (3.0 g, root of *Panax ginseng* C.A.Mey), *Cinnamomi cortex* (2.5 g, bark of *Cinnamomum cassia* Bl.), *Aurantii nobilis pericarpium* (2.0 g, peel of *Citrus unshiu* Markovich), *Polygalae radix* (2.0 g, root of *Polygala tenuifolia* Willd), *Paeoniae radix* (2.0 g, root of *Paeonia lactiflora* Pall), *Astragali radix* (1.5 g, root of *Astragalus membranaceus* Bge.), *Glycyrrhizae radix* (1.0 g, root of *Glycyrrhiza uralensis* Fisher) and *Schisandrae fructus* (1.0 g, fruit of *Schisandra chinensis* Baill). A diet containing 3% NYT was prepared by Oriental Yeast Co., Ltd. (Yokohama, Japan).

Synthetic human A β ₁₋₄₂ was purchased from China-Peptides (Shanghai, China). A β ₁₋₄₂ was dissolved in saline and used immediately when the experiments were performed. ZnAF-2DA, a membrane-permeable zinc indicator was kindly supplied from Sekisui Medical Co., LTD (Hachimantai, Japan). ZnAF-2DA is taken up into the cells through the cell membrane and is hydrolyzed by esterase in the cytosol to yield ZnAF-2 ($K_d=2.7 \times 10^{-9}$ M for Zn²⁺), which cannot permeate the cell membrane [28, 29]. The fluorescence indicator was dissolved in dimethyl sulfoxide (DMSO) and then diluted with Ringer solution containing 119 mM NaCl, 2.5 mM KCl, 1.3 mM MgSO₄, 1.0 mM NaH₂PO₄, 2.5 mM CaCl₂, 26.2 mM NaHCO₃, and 11 mM D-glucose (pH 7.3).

Animals

Male ddY mice (10 weeks of age) were purchased from Japan SLC (Hamamatsu, Japan) and caged under the standard conditions with a diurnal 12-h light cycle. The room temperature and relative humidity were controlled at 23 ± 1°C and 55 ± 5%, respectively. The mice were allowed free access to a standard laboratory diet, 3% NYT-containing diet, and water. All the experiments were performed in accordance with the Guidelines for the Care and Use of Laboratory Animals of the University of Shizuoka that refer to the American Association for Laboratory Animals Science and the guidelines laid down by the NIH (NIH Guide for the Care and Use of Laboratory Animals) in the USA. The Ethics Committee for Experimental Animals has approved this work in the University of Shizuoka.

Intracerebroventricular (ICV) injection of A β

Mice (11–13 weeks of age) were anesthetized with chloral hydrate (30 mg/kg) and placed in a stereotaxic apparatus. A microinjection canula (CXG-6, Eicom Co., Kyoto, Japan) was positioned 0.5 mm posterior to the bregma, 1.0 mm lateral, 2.2–2.4 mm inferior to the dura for ICV injection. A β ₁₋₄₂ in saline (25 μ M) was injected

via the microinjection canula at the rate of 0.5 $\mu\text{L}/\text{min}$ for 40 min (500 pmol/mouse). Ten mins later, the microinjection canula was slowly pulled up from the brain. The mice were individual housed for the experiments.

Propidium iodide (PI) staining

Fourteen days after ICV injection of $\text{A}\beta_{1-42}$, the brain was quickly removed from the mice under anesthesia and immersed in ice-cold choline-Ringer containing 124 mM choline chloride, 2.5 mM KCl, 2.5 mM MgCl_2 , 1.25 mM NaH_2PO_4 , 0.5 mM CaCl_2 , 26 mM NaHCO_3 , and 10 mM glucose (pH 7.3) to suppress excessive neuronal excitation. Coronal brain slices (400 μm) were prepared using a vibratome ZERO-1 (Dosaka Kyoto, Japan) in ice-cold choline-Ringer, which were continuously bubbled with 95% O_2 and 5% CO_2 . The brain slices were bathed in PI in Ringer solution (7 $\mu\text{g}/\text{ml}$) for 30 min, bathed in Ringer solution for 30 min and transferred to a recording chamber filled with Ringer solution. PI fluorescence (Ex/Em: 535 nm/617 nm) was captured with a confocal laser-scanning microscopic system (Nikon A1 confocal microscopes, Nikon Corp.). The region of interest was set in the dentate granule cell layer.

Fluoro-Jade B (FJB) staining

Fourteen days after ICV injection of $\text{A}\beta_{1-42}$, the mice were anesthetized with chloral hydrate and perfused with ice-cold 4% paraformaldehyde in PBS, followed by removal of the brain and overnight fixation in 4% paraformaldehyde in PBS at 4°C. Fixed brains were cryopreserved in 30% sucrose in PBS for 2 day and frozen in Tissue-Tek Optimal Cutting Temperature embedding medium. Coronal brain slices (30 μm) were prepared at -20°C in a cryostat, picked up on slides, adhered at 50°C for 60 min, and stored at -20°C . The slides were first immersed in a solution containing 1% sodium hydroxide in 80% alcohol (20 ml of 5% NaOH added to 80 ml ethanol) for 5 min. This was followed by 2 min in 70% ethanol and 2 min in distilled water. The slides were then transferred to a solution of 0.06% potassium permanganate for 15 min, preferably on a shaker table to insure consistent background suppression between slices. The slides were then rinsed in distilled water for 2 min. The staining solution was prepared from a 0.01% stock solution of FJB that was made by adding 10 mg of the dye powder to 100 ml of distilled water. The stock solution and 0.1% 4',6-diamidino-2-phenylindole (DAPI) in distilled water were diluted with 0.1% acetic acid vehicle, resulting in a final dye concentration of 0.0004% FJB and 0.0001% DAPI in the staining solution. The staining solution was prepared within 10 min of use. The slides were bathed in the staining solution for 30 min and were

rinsed for 2 min in each of three distilled water washes. Excess water was briefly removed by using a paper towel. The slides were placed at 50°C for drying. The dry slides were twice immersed in xylene for 2 min before coverslipping with DPX, a non-aqueous, non-fluorescent plastic mounting media. FJB-positive cells in the unit area were measured with a confocal laser-scanning microscopic system (Ex/Em: 480 nm/525 nm). The region of interest was set in the dentate granule cell layer.

$\text{A}\beta$ immunostaining

$\text{A}\beta_{1-42}$ (25 μM) in saline was intracerebroventricularly injected via a microinjection canula at the rate of 0.5 $\mu\text{L}/\text{min}$ for 40 min (500 pmol/mouse) of anesthetized mice as described above. One hour after the start of injection, the brain was quickly removed from the mice. For immunostaining, coronal brain slices (400 μm) were prepared using a vibratome ZERO-1 in ice-cold choline-Ringer, which were continuously bubbled with 95% O_2 and 5% CO_2 . The slices were rinsed with Ringer solution and fixed with paraformaldehyde (4% in 0.01 M PBS) for 15 min. The slices were rinsed in 0.01 M PBS three times. The slice tissues were blocked in 5% normal goat serum for 30 min, followed by rinse in 0.01M PBS three times, incubated with 70% formic acid for 5 min, rinsed with 0.01 M PBS three times, and bathed at 4°C in $\text{A}\beta$ monoclonal antibody, 4G8 (COVANCE, Burlington, NJ, USA, 1:500 dilution in 0.01M PBS) for 48 h. The slices were then rinsed with 0.01 M PBS three times, bathed in Alexa Fluor 633 goat anti-mouse IgG secondary antibody (1: 200 dilution in 0.01M PBS) for 1 h, rinsed with 0.01 M PBS three times, bathed in 0.1% DAPI in PBS for 10 min, rinsed again with 0.01 M PBS three times, and mounted on glass slides. Immunostaining images were obtained by using a confocal laser-scanning microscopic system through a $10\times$ objective. Fluorescence intensity was analyzed by the NIH Image J.

In vivo $\text{A}\beta_{1-42}$ -mediated Zn^{2+} imaging

$\text{A}\beta_{1-42}$ (25 μM) in saline containing 100 μM ZnAF-2DA was intracerebroventricularly injected via a microinjection canula at the rate of 0.5 $\mu\text{L}/\text{min}$ for 40 min (500 pmol/mouse) of anesthetized mice as described above. One hour after the start of injection, coronal brain slices (400 μm) were prepared in ice-cold choline-Ringer solution in the same manner. The brain slices were bathed in PI in Ringer solution (7 $\mu\text{g}/\text{ml}$) for 30 min, bathed in Ringer solution for 30 min and transferred to a recording chamber filled with Ringer solution. The fluorescence of ZnAF-2 (Ex/Em: 488 nm/505–530 nm) and PI (Ex/Em: 535 nm/617 nm) was captured with a confocal laser-scanning microscopic system.

MT immunostaining

A 3% NYT-containing diet was administered to mice for 2 weeks. The mice were anesthetized with chloral hydrate and perfused with ice-cold 4% paraformaldehyde in PBS, followed by removal of the brain and overnight fixation in 4% paraformaldehyde in PBS at 4°C. Fixed brains were cryopreserved in 30% sucrose in PBS for 2 day and frozen in Tissue-Tek Optimal Cutting Temperature embedding medium. Coronal brain slices (30 μ m) were prepared at -20°C in a cryostat, picked up on slides, adhered at 50°C for 60 min, and stored at -20°C. For immunostaining, the slices were first immersed in PBS for washing, incubated in blocking solution (3% BSA, 0.1% Triton X-100 in PBS) for 1 h, and rinsed with PBS for 5 min followed by overnight incubation with anti-MT antibody [UC1MT] ab12228 (Abcam, Cambridge, UK) in 0.1% Triton X-100 in PBS at 4°C. The slides were rinsed with PBS for 5 min three times and incubated in blocking buffer containing Alexa Fluor 488 goat anti-mouse secondary antibody (Thermo Fisher Scientific, Waltham, MA, USA) in 3% BSA, 0.1% Triton X-100 in PBS for 3 h at room temperature. Following three rinses in PBS for 5 min, the slides were bathed in 0.1% DAPI in PBS for 5 min, rinsed with PBS for 5 min three times, mounted with Prolong Gold antifade reagent, and placed at 4°C for 24 h. Immunostaining images were measured in the dentate gyrus using a confocal laser-scanning microscopic system.

Data analysis

Student's paired *t*-test was used for comparison of the means of paired data. For multiple comparisons, differences between treatments were assessed by one-way ANOVA followed by post hoc testing using the Tukey's test (the statistical software, GraphPad Prism 5). A value of $P < 0.05$ was considered significant. Data were expressed as means \pm SE. The results of statistical analysis are described in each figure legend.

Results

Effect of NYT on A β 1-42-induced neurodegeneration

To assess A β 1-42-induced neurodegeneration, we used PI, a fluorescent intercalating agent, which binds to DNA by intercalating between the bases with little or no sequence preference in dead cells. A diet containing 3% NYT was administered to mice for 2 weeks and human A β 1-42 was intracerebroventricularly injected. Two weeks after ICV injection of A β 1-42, PI fluorescence is significantly elevated in the dentate granule cell layer, but not in the CA1 and CA3 pyramidal cell layers [13]. Thus, PI fluorescence was determined in the dentate granule

cell layer in the present study. A β 1-42-induced elevation of PI fluorescence was reduced by administration of the diet for 4 weeks (Fig. 1). The diet did not modify the body weight of mice 4 weeks after administration (A β /control diet, 34.1 \pm 0.7 g; A β /NYT-containing diet, 34.9 \pm 0.9 g).

A β 1-42 readily captures extracellular Zn²⁺ and Zn-A β 1-42 complexes formed is rapidly taken up into dentate gyrus neurons [9, 30]. It is estimated that A β 1-42-induced neurodegeneration is closely linked with Zn²⁺ release from intracellular Zn-A β 1-42 complexes [13]. To see the effect of NYT pre-administration, we checked the levels of A β 1-42 and Zn²⁺ in the dentate granule cell layer after pre-administration of the diet for 2 weeks. A β staining (uptake) was not modified even after pre-administration of the diet for 2 weeks and there was no significant difference between A β group and A β + NYT group (Fig. 2). In contrast, A β 1-42-induced increase in intracellular Zn²⁺ was reduced after pre-administration of the diet and there was a significant difference between A β group and A β + NYT group (Fig. 3). These data suggest that pre-administration of NYT prior to A β injection is effective for reducing intracellular Zn²⁺ toxicity induced by A β 1-42.

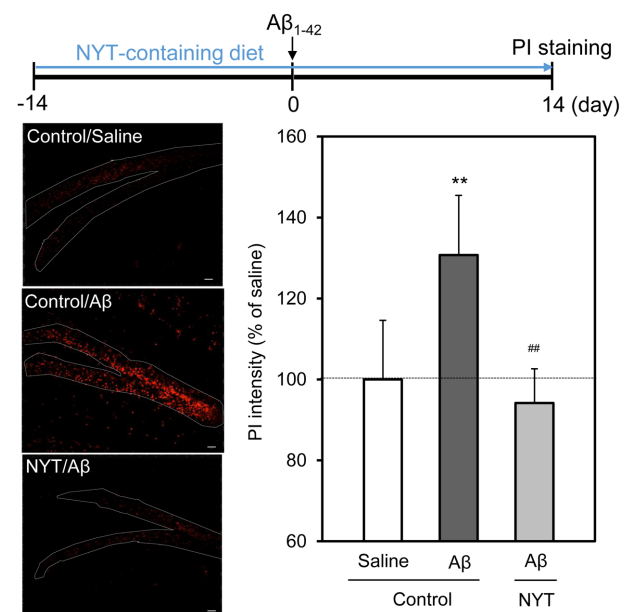


Fig. 1. A β 1-42-induced neurodegeneration determined by propidium iodide (PI) staining is rescued after Ninjin-yoei-to (NYT) administration for 4 weeks. Four weeks after administration of the NYT-containing diet (upper), PI fluorescence was measured in the dentate granule cell layer surrounded by the dotted line (lower-left). Bar; 50 μ m. Each bar and line (mean \pm SEM) represent the rate (%) of PI fluorescence after A β 1-42 injection to that after saline (vehicle) injection, which was represented as 100% (lower-right). ** $P < 0.01$, vs. saline, ## $P < 0.01$, vs. A β (Tukey's test). saline, n=18; A β , n=32; A β /NYT, n=18.

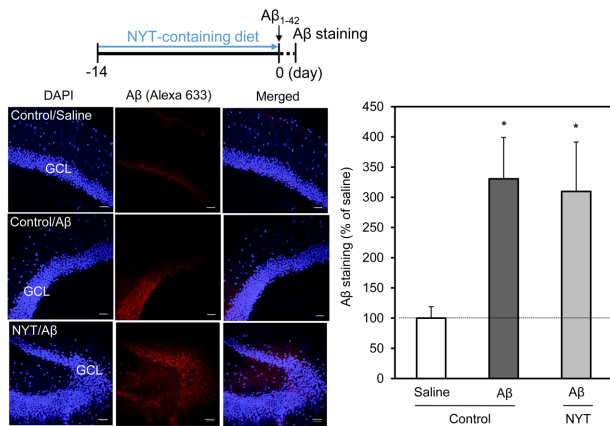


Fig. 2. $A\beta_{1-42}$ uptake in the dentate gyrus is not modified after Ninjin-yoei-to (NYT) pre-administration for 2 weeks. The NYT-containing diet was administered to mice for 2 weeks and $A\beta_{1-42}$ was intracerebroventricularly injected into the mice (upper). One hour after the start of injection, $A\beta$ immunostaining was determined in the dentate granule cell layer (GCL) (lower-left). Bar; 50 μ m. Each bar and line (mean \pm SEM) represent the rate (%) of $A\beta$ staining after $A\beta_{1-42}$ injection to that after saline (vehicle) injection, which was represented as 100% (lower-right). * $P < 0.05$, vs. saline (Tukey's test). saline, $n = 6$; $A\beta$, $n = 3$; $A\beta$ /NYT, $n = 3$.

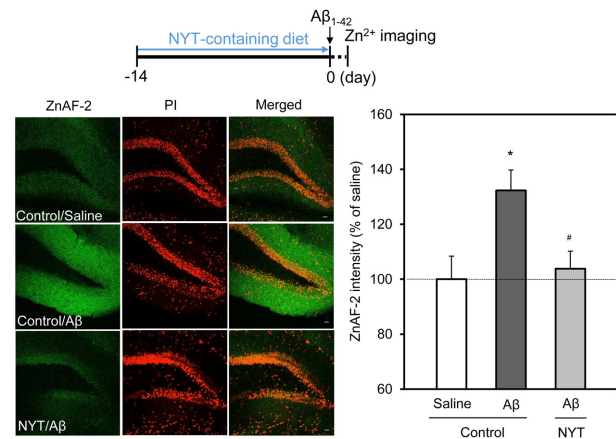


Fig. 3. $A\beta_{1-42}$ -induced increase in intracellular Zn^{2+} in the dentate gyrus is reduced after Ninjin-yoei-to (NYT) pre-administration for 2 weeks. The NYT-containing diet was administered to mice for 2 weeks and $A\beta_{1-42}$ was intracerebroventricularly injected into the mice (upper). One hour after the start of injection, intracellular ZnAF-2 fluorescence was determined in the dentate granule cell layer (lower-left). Bar; 50 μ m. Each bar and line (mean \pm SEM) represent the rate (%) of ZnAF-2 fluorescence after $A\beta_{1-42}$ injection to that after saline (vehicle) injection, which was represented as 100% (lower-right). * $P < 0.05$, vs. saline; # $P < 0.05$, vs. $A\beta$ (Tukey's test). saline, $n = 10$; $A\beta$, $n = 28$; $A\beta$ /NYT, $n = 18$.

Rescuing effect of NYT-induced MT synthesis on $A\beta_{1-42}$ -induced neurodegeneration

PI fluorescence was also checked by pre-administration of the NYT-containing diet for 2 weeks (Fig. 4). $A\beta_{1-42}$ -induced elevation of PI fluorescence was reduced in agreement with the case of administration of the diet for 4 weeks (Fig. 1). There was also a significant difference between $A\beta$ group and $A\beta$ + NYT group (Fig. 4). To confirm $A\beta_{1-42}$ -induced neurodegeneration, we used FJB, an anionic fluorescein derivative, which is used for the histological staining of neurons undergoing degeneration. $A\beta_{1-42}$ -induced increase in FJB-positive cells was reduced by pre-administration of the NYT-containing diet (Fig. 5).

MTs is a candidate, which reduces increase in intracellular Zn^{2+} without modifying intracellular $A\beta_{1-42}$ level [10, 13]. We checked the level of MTs after administration of the NYT-containing diet for 2 weeks. The level of MTs was increased in the dentate granule cell layer after the administration (Fig. 6).

Discussion

When the concentration of human $A\beta_{1-42}$ reaches 100–500 pM in the extracellular compartment of the rat hippocampus, Zn - $A\beta_{1-42}$ complexes are formed extracellularly Zn^{2+} -dependently [9]. Zn - $A\beta_{1-42}$ complexes are rapidly taken up into dentate gyrus neurons in synaptic

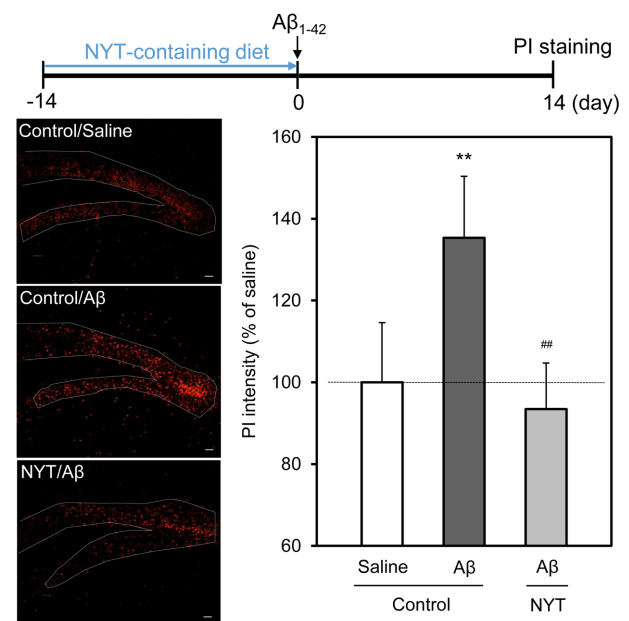


Fig. 4. $A\beta_{1-42}$ -induced neurodegeneration determined by propidium iodide (PI) staining is rescued after Ninjin-yoei-to (NYT) pre-administration for 2 weeks. Two weeks after administration of the NYT-containing diet, $A\beta_{1-42}$ was intracerebroventricularly injected into mice (upper). Two weeks later, PI fluorescence was measured in the dentate granule cell layer surrounded by the dotted line (lower-left). Bar; 50 μ m. Each bar and line (mean \pm SEM) represent the rate (%) of PI fluorescence after $A\beta_{1-42}$ injection to that after saline (vehicle) injection, which was represented as 100% (lower-right). ** $P < 0.01$, vs. saline, ## $P < 0.01$, vs. $A\beta$ (Tukey's test). saline, $n = 18$; $A\beta$, $n = 25$; $A\beta$ /NYT, $n = 9$.

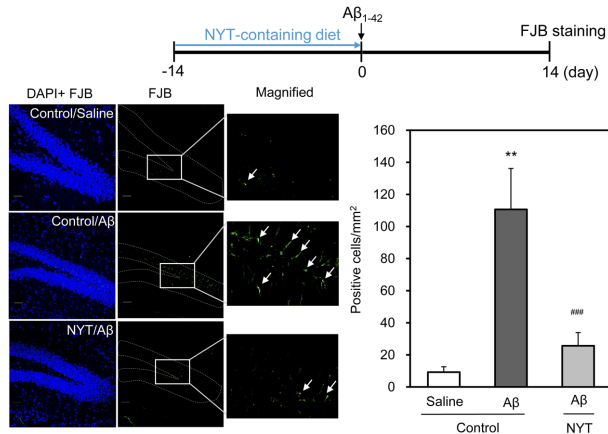


Fig. 5. A β ₁₋₄₂-induced neurodegeneration determined by Fluoro-Jade B (FJB) staining is also rescued after Ninjin-yoei-to (NYT) pre-administration for 2 weeks. Two weeks after administration of the NYT-containing diet, A β ₁₋₄₂ was intracerebroventricularly injected into mice (upper). Two weeks later, FJB fluorescence was measured in the dentate granule cell layer surrounded by the dotted line (lower-left). Bar; 50 μ m. Each bar and line (mean \pm SEM) represent FJB-positive cells in the unit area after injection of vehicle and A β ₁₋₄₂. (lower-right). ** P <0.01, vs. saline, ### P <0.001, vs. A β (Tukey's test). saline, n=12; A β , n=32; A β /NYT, n=24.

activity-independent manner [30]. On the other hand, A β ₁₋₄₂ is less taken up into CA3 and CA1 neurons [30] followed by less neurodegeneration in the CA3 and CA1 [13]. However, intracellular Zn²⁺ is significantly increased in the CA3 and CA1 as well as the dentate gyrus [13]. It is estimated that the rapid uptake of A β ₁₋₄₂ into dentate gyrus neurons is involved in the preferential neurodegeneration in the hippocampus, which may be linked with the A β ₁₋₄₂-mediated pathogenesis. In the present study, we focused on vulnerability of dentate gyrus neurons to A β ₁₋₄₂-induced intracellular Zn²⁺ toxicity. Neurodegeneration in the dentate granule cell layer, which was determined 2 weeks after intracerebroventricular injection of A β ₁₋₄₂, was rescued by administration of a diet containing 3% NYT for 4 weeks.

A β ₁₋₄₂-induced neurodegeneration is rescued by co-injection of extracellular (CaEDTA) and intracellular (ZnAF-2DA) Zn²⁺ chelators [13], suggesting that Zn²⁺ release from intracellular Zn-A β ₁₋₄₂ complexes leads to neurodegeneration. It is estimated that the death signaling via Zn²⁺ emerges in a short period after the uptake of Zn-A β ₁₋₄₂ complexes into neurons [13]. A β staining (uptake) was not modified in the dentate granule cell layer by pre-administration of the NYT-containing diet for 2 weeks, while A β ₁₋₄₂-induced increase in intracellular Zn²⁺ was reduced, suggesting that pre-administration of NYT prior to A β ₁₋₄₂ injection is effective for reducing A β ₁₋₄₂-induced Zn²⁺ toxicity. When the preventive

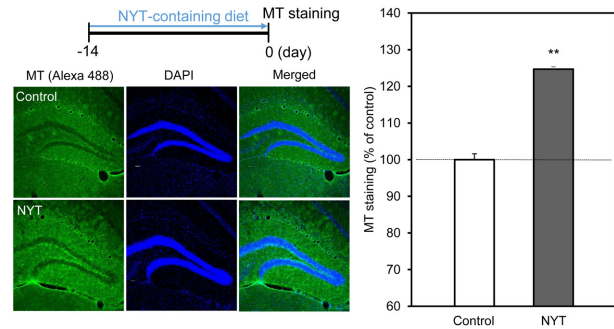


Fig. 6. Metallothionein (MT) level in the dentate gyrus is elevated after Ninjin-yoei-to (NYT) administration for 2 weeks. The NYT-containing diet was administered to mice for 2 weeks (left-upper). MT immunostaining was determined in the dentate granule cell layer (left-lower). Bar; 50 μ m. Each bar and line (mean \pm SEM) represent the rate (%) of MT staining after NYT administration to that after the control diet administration, which was represented as 100% (right). ** P <0.01, vs. control (t -test). Control, n=8; NYT, n=12.

effect of the NYT-containing diet was checked, A β ₁₋₄₂-induced neurodegeneration was rescued by pre-administration of NYT. *In vivo* LTP at the perforant pathway-dentate granule cell synapses is affected after local injection of A β ₁₋₄₂ into the dentate granule cell layer, but not by preinjection of MT-I and MT-II inducers, i.e., Zn, Cd, and corticosterone, into the dentate granule cell layer prior to A β ₁₋₄₂ injection [10]. Furthermore, A β ₁₋₄₂ uptake is not modified in the dentate granule cell layer by pretreatment with dexamethasone, an inducer of MT-I and MT-II, while A β ₁₋₄₂-induced increase in intracellular Zn²⁺ is reduced, resulting in rescuing the affected LTP [10]. A β ₁₋₄₂-induced neurodegeneration is also rescued in the dentate gyrus by the pretreatment with dexamethasone, which reduced A β ₁₋₄₂-induced increase in intracellular Zn²⁺ [13]. These data indicate that Zn²⁺ release from intracellular Zn-A β ₁₋₄₂ complexes contributes to neurotoxicity rather than A β ₁₋₄₂ itself. We postulated that NYT contains novel inducers of MTs, which can capture Zn²⁺ from intracellular Zn-A β ₁₋₄₂ complexes. As a matter of fact, the level of MTs was increased in the dentate granule cell layer by pre-administration of NYT prior to A β injection. A variety of MT inducer has been reported in the peripheral tissues [31], while limited MT inducers are known in the brain because most MT inducers do not pass through the blood-brain barrier [32]. Synthetic adrenocortical hormones, e.g., dexamethasone induces MT in the brain after intraperitoneal injection [10], but they have serious side effects after chronic administration. Secure substances to induce MTs in the brain by oral administration are unknown. In Kampo medicines, Juzen-taiho-to (JTX) is used for adjunctive treatment of cancers and autoimmune diseases. JTX enhances expres-

sion of MT-I and -II significantly in the liver of mice, suggesting that MTs mediate at least some effects of JTX in mice [33]. Unfortunately, there is no evidence on MT induction in the brain by Kampo medicines and no attention has been paid to MT induction in the brain by Kampo medicines. In the present study, it is likely that NYT contains secure substances to induce MTs in the brain. NYT has been traditionally used for the patients with anorexia, insomnia, neurosis [34], suggesting that some NYT components pass through the blood-brain barrier and can induce MTs in the brain. On the other hand, polyphenols can chelate Zn^{2+} [35] and it is possible that some NYT components directly capture Zn^{2+} released from $A\beta_{1-42}$.

MTs can capture 7 equivalents of Zn^{2+} , resulting in the holo-MTs, Zn_7 MTs. The zinc-binding sites of MTs vary affinities for Zn^{2+} [36–38] and intracellular MTs are mainly the form of Zn_5 MTs when intracellular Zn^{2+} concentration is approximately 100 pM, an estimated basal concentration [39]. On the other hand, MTs are the form of Zn_7 MTs when intracellular Zn^{2+} concentration is approximately 10 nM, an estimated concentration in the extracellular compartment [40]. The rapid influx of extracellular Zn^{2+} into the intracellular compartment, which is induced by producing extracellular Zn - $A\beta_{1-42}$ complexes, leads to the saturation of zinc-binding capacity of MTs followed by $A\beta_{1-42}$ -induced intracellular Zn^{2+} toxicity (Fig. 7). Thus, it is estimated that an increase in MTs is effective for buffering the rapid increase in free Zn^{2+} by $A\beta_{1-42}$ in the intracellular compartment. *In vivo* K_d value of Zn^{2+} to $A\beta_{1-42}$ may be in the range of ~3–30

nM [9], which is higher than that of MTs (~1 pM) under the physiological condition [41]. When MTs capture Zn^{2+} in the liver, the biological half-life is estimated to be 18–20 h [42]. Thus, it is estimated that the maximum level of induced MTs may be reached in a few days after NYT administration.

In conclusion, the present study indicates that pre-administration of NYT prevents $A\beta_{1-42}$ -mediated neurodegeneration in the hippocampus by induced synthesis of MTs, which reduces intracellular Zn^{2+} toxicity induced by $A\beta_{1-42}$. NYT may be effective for AD via preventing $A\beta_{1-42}$ -induced pathogenesis. Although it is unknown whether administration of the NYT-containing diet modifies the cholinergic system, it is estimated that the modification is not linked with induction of MT synthesis. It remains to find out novel inducers of MTs in NYT and also clarify the mechanism of MT induction.

Conflicts of Interest

Authors declare no conflicts of interest.

References

1. Scheff SW, Price DA, Schmitt FA, Mufson EJ. Hippocampal synaptic loss in early Alzheimer's disease and mild cognitive impairment. *Neurobiol Aging*. 2006; 27: 1372–1384. [Medline] [CrossRef]
2. Crews L, Masliah E. Molecular mechanisms of neurodegeneration in Alzheimer's disease. *Hum Mol Genet*. 2010; 19:(R1): R12–R20. [Medline] [CrossRef]
3. Small SA, Schobel SA, Buxton RB, Witter MP, Barnes CA. A pathophysiological framework of hippocampal dysfunction in ageing and disease. *Nat Rev Neurosci*. 2011; 12: 585–601. [Medline] [CrossRef]
4. Morys J, Sadowski M, Barcikowska M, Maciejewska B, Narkiewicz O. The second layer neurons of the entorhinal cortex and the perforant path in physiological ageing and Alzheimer's disease. *Acta Neurobiol Exp (Warsz)*. 1994; 54: 47–53. [Medline]
5. Gómez-Isla T, Price JL, McKeel DW Jr, Morris JC, Growdon JH, Hyman BT. Profound loss of layer II entorhinal cortex neurons occurs in very mild Alzheimer's disease. *J Neurosci*. 1996; 16: 4491–4500. [Medline] [CrossRef]
6. Harris JA, Devidze N, Verret L, Ho K, Halabisky B, Thwin MT, et al. Transsynaptic progression of amyloid- β -induced neuronal dysfunction within the entorhinal-hippocampal network. *Neuron*. 2010; 68: 428–441. [Medline] [CrossRef]
7. Qin Y, Tian Y, Han H, Liu L, Ge X, Xue H, et al. Alzheimer's Disease Neuroimaging Initiative. Risk classification for conversion from mild cognitive impairment to Alzheimer's disease in primary care. *Psychiatry Res*. 2019; 278: 19–26. [Medline] [CrossRef]
8. Takeda A, Nakamura M, Fujii H, Uematsu C, Minamino T, Adlard PA, et al. Amyloid β -mediated Zn^{2+} influx into dentate granule cells transiently induces a short-term cognitive deficit. *PLoS One*. 2014; 9: e115923. [Medline] [CrossRef]
9. Takeda A, Tamano H, Tempaku M, Sasaki M, Uematsu C, Sato S, et al. Extracellular Zn^{2+} is essential for amyloid β_{1-42} -induced cognitive decline in the normal brain and its rescue. *J Neurosci*. 2017; 37: 7253–7262. [Medline] [CrossRef]
10. Takeda A, Tamano H, Hashimoto W, Kobuchi S, Suzuki H,

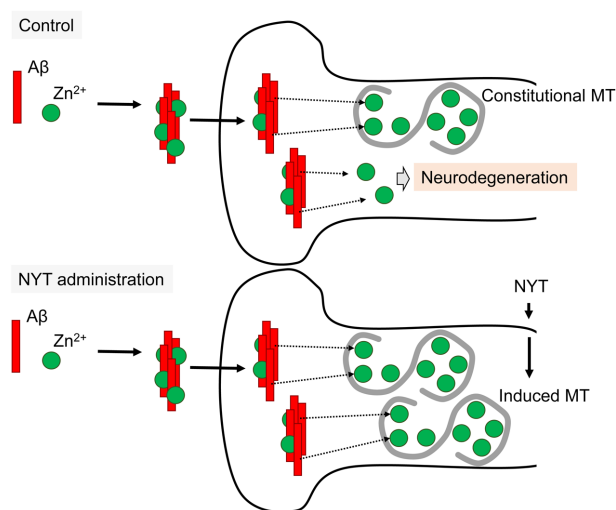


Fig. 7. Proposed rescue mechanism of Ninjin-yoei-to (NYT) via induced synthesis of MTs on $A\beta_{1-42}$ -induced neurodegeneration via intracellular Zn^{2+} toxicity. $A\beta_{1-42}$ uptake into dentate gyrus neurons play a key role for $A\beta_{1-42}$ -mediated pathogenesis, in which Zn^{2+} toxicity via the uptake is crucial (upper) [9].

- Murakami T, et al. Novel defense by metallothionein induction against cognitive decline: from amyloid β_{1-42} -induced excess Zn^{2+} to functional Zn^{2+} deficiency. *Mol Neurobiol*. 2018; 55: 7775–7788. [Medline] [CrossRef]
11. Sensi SL, Canzoniero LM, Yu SP, Ying HS, Koh JY, Kerchner GA, et al. Measurement of intracellular free zinc in living cortical neurons: routes of entry. *J Neurosci*. 1997; 17: 9554–9564. [Medline] [CrossRef]
 12. Colvin RA, Bush AI, Volitakis I, Fontaine CP, Thomas D, Kikuchi K, et al. Insights into Zn^{2+} homeostasis in neurons from experimental and modeling studies. *Am J Physiol Cell Physiol*. 2008; 294: C726–C742. [Medline] [CrossRef]
 13. Tamano H, Takiguchi M, Tanaka Y, Murakami T, Adlard PA, Bush AI, et al. Preferential neurodegeneration in the dentate gyrus by amyloid β_{1-42} -induced intracellular Zn^{2+} dysregulation and its defense strategy. *Mol Neurobiol*. 2020; 57: 1875–1888. [Medline] [CrossRef]
 14. Iwasaki K, Satoh-Nakagawa T, Maruyama M, Monma Y, Nemoto M, Tomita N, et al. A randomized, observer-blind, controlled trial of the traditional Chinese medicine Yi-Gan San for improvement of behavioral and psychological symptoms and activities of daily living in dementia patients. *J Clin Psychiatry*. 2005; 66: 248–252. [Medline] [CrossRef]
 15. Matsuda Y, Kishi T, Shibayama H, Iwata N. Yokukansan in the treatment of behavioral and psychological symptoms of dementia: a systematic review and meta-analysis of randomized controlled trials. *Hum Psychopharmacol*. 2013; 28: 80–86. [Medline] [CrossRef]
 16. Monji A, Takita M, Samejima T, Takaishi T, Hashimoto K, Matsunaga H, et al. Effect of yokukansan on the behavioral and psychological symptoms of dementia in elderly patients with Alzheimer's disease. *Prog Neuropsychopharmacol Biol Psychiatry*. 2009; 33: 308–311. [Medline] [CrossRef]
 17. Okamoto H, Iyo M, Ueda K, Han C, Hirasaki Y, Namiki T. Yokukan-san: a review of the evidence for use of this Kampo herbal formula in dementia and psychiatric conditions. *Neuropsychiatr Dis Treat*. 2014; 10: 1727–1742. [Medline] [CrossRef]
 18. Kudoh C, Arita R, Honda M, Kishi T, Komatsu Y, Asou H, et al. Effect of ninjin'yoeito, a Kampo (traditional Japanese) medicine, on cognitive impairment and depression in patients with Alzheimer's disease: 2 years of observation. *Psychogeriatrics*. 2016; 16: 85–92. [Medline] [CrossRef]
 19. Kiyohara H, Matsumoto T, Yabe T, Yamada H. Comparison of effects on immune system and central nervous system of Juzen-taiho-to and Ninjin-yoei-to. *J Trad Med*. 1997; 14: 456–457.
 20. Toriizuka K, Iijima K, Yabe T, Cyong JC. Effects of Kampo prescriptions on the neural-immune functions of ovariectomized mice (V). *J Trad Med*. 1994; 11: 386–387.
 21. Egashira N, Yuzurihara M, Hattori N, Sakakibara I, Ishige A. Ninjin-yoei-to (Ren-Shen-Yang-Rong-Tang) and Polygalae radix improves scopolamine-induced impairment of passive avoidance response in mice. *Phytomedicine*. 2003; 10: 467–473. [Medline] [CrossRef]
 22. Davies P, Maloney AJ. Selective loss of central cholinergic neurons in Alzheimer's disease. *Lancet*. 1976; 2: 1403. [Medline] [CrossRef]
 23. Bartus RT, Dean RL 3rd, Beer B, Lippa AS. The cholinergic hypothesis of geriatric memory dysfunction. *Science*. 1982; 217: 408–414. [Medline] [CrossRef]
 24. Whitehouse PJ, Price DL, Struble RG, Clark AW, Coyle JT, Delon MR. Alzheimer's disease and senile dementia: loss of neurons in the basal forebrain. *Science*. 1982; 215: 1237–1239. [Medline] [CrossRef]
 25. Summers WK, Majovski LV, Marsh GM, Tachiki K, Kling A. Oral tetrahydroaminoacridine in long-term treatment of senile dementia, Alzheimer type. *N Engl J Med*. 1986; 315: 1241–1245. [Medline] [CrossRef]
 26. Rogers SL, Farlow MR, Doody RS, Mohs R, Friedhoff LT. Donepezil Study Group. A 24-week, double-blind, placebo-controlled trial of donepezil in patients with Alzheimer's disease. *Neurology*. 1998; 50: 136–145. [Medline] [CrossRef]
 27. Yabe T, Tuchida H, Kiyohara H, Takeda T, Yamada H. Induction of NGF synthesis in astrocytes by onjisaponins of Polygala tenuifolia, constituents of kampo (Japanese herbal) medicine, Ninjin-yoei-to. *Phytomedicine*. 2003; 10: 106–114. [Medline] [CrossRef]
 28. Hirano T, Kikuchi K, Urano Y, Nagano T. Improvement and biological applications of fluorescent probes for zinc, ZnAFs. *J Am Chem Soc*. 2002; 124: 6555–6562. [Medline] [CrossRef]
 29. Ueno S, Tsukamoto M, Hirano T, Kikuchi K, Yamada MK, Nishiyama N, et al. Mossy fiber Zn^{2+} spillover modulates heterosynaptic *N*-methyl-*D*-aspartate receptor activity in hippocampal CA3 circuits. *J Cell Biol*. 2002; 158: 215–220. [Medline] [CrossRef]
 30. Tamano H, Oneta N, Shioya A, Adlard PA, Bush AI, Takeda A. In vivo synaptic activity-independent co-uptakes of amyloid β_{1-42} and Zn^{2+} into dentate granule cells in the normal brain. *Sci Rep*. 2019; 9: 6498. [Medline] [CrossRef]
 31. Haq F, Mahoney M, Koropatnick J. Signaling events for metallothionein induction. *Mutat Res*. 2003; 533: 211–226. [Medline] [CrossRef]
 32. Ebadi M, Iversen PL, Hao R, Cerutis DR, Rojas P, Happe HK, et al. Expression and regulation of brain metallothionein. *Neurochem Int*. 1995; 27: 1–22. [Medline] [CrossRef]
 33. Anjiki N, Hoshino R, Ohnishi Y, Hioki K, Irie Y, Ishige A, et al. A Kampo formula Juzen-taiho-to induces expression of metallothioneins in mice. *Phytother Res*. 2005; 19: 915–917. [Medline] [CrossRef]
 34. Goswami C, Dezaki K, Wang L, Inui A, Seino Y, Yada T. Ninjin-yoeito activates ghrelin-responsive and unresponsive NPY neurons in the arcuate nucleus and counteracts cisplatin-induced anorexia. *Neuropeptides*. 2019; 75: 58–64. [Medline] [CrossRef]
 35. Dabbagh-Bazarbachi H, Clergeaud G, Quesada IM, Ortiz M, O'Sullivan CK, Fernández-Larrea JB. Zinc ionophore activity of quercetin and epigallocatechin-gallate: from Hepa 1-6 cells to a liposome model. *J Agric Food Chem*. 2014; 62: 8085–8093. [Medline] [CrossRef]
 36. Krężel A, Maret W. Zinc-buffering capacity of a eukaryotic cell at physiological pZn. *J Biol Inorg Chem*. 2006; 11: 1049–1062. [Medline] [CrossRef]
 37. Krężel A, Hao Q, Maret W. The zinc/thiolate redox biochemistry of metallothionein and the control of zinc ion fluctuations in cell signaling. *Arch Biochem Biophys*. 2007; 463: 188–200. [Medline] [CrossRef]
 38. Krężel A, Maret W. Dual nanomolar and picomolar Zn(II) binding properties of metallothionein. *J Am Chem Soc*. 2007; 129: 10911–10921. [Medline] [CrossRef]
 39. Krężel A, Maret W. The Functions of Metamorphic Metallothioneins in Zinc and Copper Metabolism. *Int J Mol Sci*. 2017; 18: 1237. [CrossRef]. [Medline]
 40. Frederickson CJ, Giblin LJ, Krezel A, McAdoo DJ, Mueller RN, Zeng Y, et al. Concentrations of extracellular free zinc (pZn) in the central nervous system during simple anesthetization, ischemia and reperfusion. *Exp Neurol*. 2006; 198: 285–293. [Medline] [CrossRef]
 41. Vasák M, Káři JH. Spectroscopic properties of metallothionein. In *Metal Ions in Biological Systems*. Sigel H. Ed., Marcel Dekker, New York, NY, USA, Volume 15, pp. 213–273 (1983).
 42. Cousins RJ. Metallothionein synthesis and degradation: relationship to cadmium metabolism. *Environ Health Perspect*. 1979; 28: 131–136. [Medline] [CrossRef]